Macrophage mTORC1 disruption reduces inflammation and insulin resistance in obese mice

Jiang, Hongfeng; Westerterp, Marit; Wang, Chunjiong; Zhu, Yi; Ai, Ding

Published in:
Diabetologia

DOI:
10.1007/s00125-014-3350-5

Publication date:
2014

Diabetologia (2014) 57:2393–2404
DOI 10.1007/s00125-014-3350-5

ARTICLE

Macrophage mTORC1 disruption reduces inflammation and insulin resistance in obese mice

Hongfeng Jiang · Marit Westerterp · Chunjiong Wang · Yi Zhu · Ding Ai

Received: 21 April 2014 / Accepted: 16 July 2014 / Published online: 14 August 2014

Abstract

Aims/hypothesis Inflammatory factors secreted by macrophages play an important role in obesity-related insulin resistance. Being at the crossroads of a nutrient–hormonal signalling network, the mammalian target of rapamycin complex 1 (mTORC1) controls important functions in the regulation of energy balance and peripheral metabolism. However, the role of macrophage mTORC1 in insulin resistance is still unclear. In the current study, we investigated the physiological role of macrophage mTORC1 in regulating inflammation and insulin sensitivity.

Methods We generated mice deficient in the regulatory associated protein of mTOR (Raptor) in macrophages, by crossing *Raptor* (also known as *Rptor*) floxed mice (*Raptor*$^{flox/flox}$) with mice expressing Cre recombinase under the control of the Lysm-Cre promoter (*Mac-Raptor*^{KO}). We fed mice chow or high-fat diet (HFD) and assessed insulin sensitivity in liver, muscle and adipose tissue. Subsequently, we measured inflammatory gene expression in liver and adipose tissue and investigated the role of Raptor deficiency in the regulation of inflammatory responses in peritoneal macrophages from HFD-fed mice or in palmitic acid-stimulated bone marrow-derived macrophages (BMDMs).

Results Mac-Raptor^{KO} mice fed HFD had improved systemic insulin sensitivity compared with *Raptor*$^{flox/flox}$ mice. Macrophage Raptor deficiency reduced inflammatory gene expression in liver and adipose tissue, fatty liver and adipose tissue macrophage content in response to HFD. In peritoneal macrophages from mice fed with an HFD for 12 weeks, macrophage Raptor deficiency decreased inflammatory gene expression, through attenuation of the inactivation of Akt and subsequent inhibition of the inositol-requiring element 1α/clun NH_2-terminal kinase–nuclear factor kappa-light-chain-enhancer of activated B cells (IRE1α/JNK/NFκB) pathways. Similarly, mTOR inhibition as a result of Raptor deficiency or rapamycin treatment decreased palmitic acid-induced inflammatory gene expression in BMDMs in vitro.

Conclusions/interpretation The disruption of mTORC1 signalling in macrophages protects mice against inflammation and insulin resistance potentially by inhibiting HFD- and palmitic acid-induced IRE1α/JNK/NFκB pathway activation.

Keywords Inflammation · Insulin resistance · mTORC1

Abbreviations

ATF6	Activating transcription factor 6
ATM	Adipose tissue macrophage
BMDM	Bone marrow-derived macrophage
CD	Chow diet
ConA	Concanavalin A
DIO	Diet-induced obesity
eIF2α	Eukaryotic translation initiation factor 2α
ER	Endoplasmic reticulum
HFD	High-fat diet
IPGTT	Intraperitoneal glucose tolerance test
IPITT	Intraperitoneal insulin tolerance test
IRE1α	Inositol-requiring element 1α

Electronic supplementary material The online version of this article (doi:10.1007/s00125-014-3350-5) contains peer-reviewed but unedited supplementary material, which is available to authorised users.

H. Jiang · M. Westerterp · D. Ai
Division of Molecular Medicine, Department of Medicine, Columbia University, New York, NY, USA

M. Westerterp
Department of Medical Biochemistry, Academic Medical Center, University of Amsterdam, Amsterdam, The Netherlands

C. Wang · Y. Zhu · D. Ai (✉)
Department of Physiology and Pathophysiology, Tianjin Medical University, 300070 Tianjin, People's Republic of China
e-mail: edin2000cn@gmail.com

JNK	cJun NH_2-terminal kinase
mTORC1/2	Mammalian target of rapamycin complex 1/2
NF-κB	Nuclear factor κB
NMR	Nuclear magnetic resonance
PERK	RNA-dependent protein kinase-like ER kinase
p70S6k	p70 S6 kinase
Raptor	Regulatory associated protein of mTOR
SFA	Saturated fatty acid
TG	Triacylglycerol
TLR	Toll-like receptor
UPR	Unfolded protein response
WAT	White adipose tissue
XBP1	X box binding protein 1

Introduction

Over recent decades, it has become clear that obesity is associated with the activation of endoplasmic reticulum (ER) stress signalling and inflammatory pathways, which contribute to obesity-related cardiovascular disease, metabolic syndrome and type 2 diabetes [1–3]. ER stress signalling, which is referred to as the unfolded protein response (UPR), is triggered by three downstream proteins, inositol-requiring element 1α (IRE1α), activating transcription factor 6 (ATF6) and RNA-dependent protein kinase-like ER kinase (PERK). Among these three pathways, the IRE1α–X box binding protein 1 (XBP1) branch has been implicated in obesity-induced insulin resistance and type 2 diabetes [3–5]. In obesity, tissue macrophages, which accumulate in adipose tissue and liver, are in an inflammatory state, and are the major source of local inflammation and insulin resistance [6–8]. In macrophages, the cJun NH_2-terminal kinase (JNK) signalling pathway mediates inflammatory factor production and plays a key role in establishing obesity-induced insulin resistance [9, 10]. Saturated fatty acids (SFA) are systemically elevated in diet-induced obesity (DIO) [11, 12] and trigger inflammation and apoptosis in macrophages through ER stress [13, 14]. This stimulation is mediated, at least in part, by signalling through Toll-like receptor (TLR) 2 and TLR4 and the associated activation of JNK [12].

Mammalian target of rapamycin complex 1 (mTORC1) acts as a hub, which integrates several environmental cues such as nutritional stimuli and regulates many cellular processes including autophagy, protein translation and ribosomal biogenesis [15]. The mTORC1 is composed of mTOR, regulatory associated protein of mTOR (Raptor) and mLST8, and is sensitive to rapamycin. mTORC1 is one of the key regulators for cell growth and metabolism through mTORC1-mediated direct phosphorylation of ribosomal p70 S6 kinase (p70S6K) and eukaryotic initiation factor 4E (eIF4E)-binding protein. Rapamycin has been suggested for the treatment of mTORC1-related diseases, including cancer, cardiovascular diseases and metabolic disorders [16]. Interestingly, these diseases are also considered to be ER stress-related disorders. In the liver, genetic and diet-induced long-term activation of mTORC1 causes ER stress [17] and results in metabolic disorders [18]. ER stress intersects with many different inflammatory signalling pathways [19]. However, the function of macrophage mTORC1 in inflammatory response and insulin resistance caused by obesity-related ER stress remains unknown. In this study, we set out to examine the role of macrophage mTORC1 in insulin resistance and the mechanisms involved. For our studies, we crossed *Raptor* (also known as *Rptor*) floxed (*Raptor*$^{flox/flox}$) mice with Lysm-Cre mice, generating Lysm-Cre*Raptor*$^{flox/flox}$ mice, which we will refer to as *Mac-Raptor*^{KO} mice. We found that *Mac-Raptor*^{KO} mice had decreased mTORC1 activity in macrophages. *Mac-Raptor*^{KO} and control *Raptor*$^{flox/flox}$ mice were fed a high-fat diet (HFD) to induce insulin resistance. On an HFD, *Mac-Raptor*^{KO} mice displayed improved insulin sensitivity and reduced inflammatory factor expression in liver and adipose tissue. Mechanistical studies showed that this may be due to decreased macrophage inflammatory gene expression via attenuation of IRE1α/JNK/nuclear factor κB (NF-κB) pathway activation.

Methods

Animals and diet *Raptor*$^{flox/flox}$ mice (stock No. 013188; The Jackson Laboratory, Bar Harbor, ME, USA) were mated with transgenic mice expressing Cre recombinase under the control of the Lysm promoter (Lysm-Cre; stock No. 004781; Jackson Laboratories) to generate mice with or without *Raptor* (*Mac-Raptor*^{KO}) expression in myeloid cells. *Raptor*$^{flox/flox}$ littermates without the Cre recombinase transgene were used as controls throughout the study. Male mice (8 weeks old) were fed an HFD (60% of energy from fat; D12492i; Research Diets, New Brunswick, NJ, USA) or chow diet (CD; diet 5053; Purina Mills, Gray Summit, MO, USA) for 12 weeks. Mice were killed 10 min after i.p. injection of PBS or insulin (0.75 U/kg body weight). Body composition measurements were performed with the miniSpec TD NMR analyzer (Bruker, Billerica, MA, USA). All protocols were approved by the Institutional Animal Care and Use Committee of Columbia University. Principles of Laboratory Animal Care (NIH publication no. 85–23, revised 1985; http://grants1.nih.gov/grants/olaw/references/phspol.htm, accessed 1 January 2012) were followed.

Metabolic analyses We measured blood glucose concentration by glucose meter (OneTouch, Milpitas, CA, USA) and plasma insulin concentration by ELISA (Millipore, Temecula, CA, USA) for intraperitoneal glucose tolerance (IPGTT), intraperitoneal insulin tolerance (IPITT) and fasting/re-feeding tests. We performed the IPGTT after a 16 h fast (18:00 hours to 10:00 hours) using an i.p. injection of 2 g per kg body weight glucose. For the IPITT, fasting blood glucose was measured (4 h fast, blood taken from the tail vein). Insulin was then injected intraperitoneally (0.75 U/kg) and blood glucose was measured again at time points of 30, 60, 90 and 120 min, post injection. For fasting/re-feeding studies, mice were fasted for 16 h and blood was collected. Mice were then re-fed for the indicated time. A small piece of liver was taken, weighed and homogenised. Next, we extracted hepatic lipids, measured triaglycerol (TG) levels, and normalised them to tissue weight. To measure TG and cholesterol content, colorimetric assays from Thermo (Waltham, MA, USA) and Wako (Richmond, VA, USA), respectively, were used.

Macrophage culture See electronic supplementary material (ESM) Methods for details.

Real-time quantitative PCR analysis See ESM Methods for details.

Western blot analysis See ESM Methods for details.

Immunohistochemistry See ESM Methods for details.

Statistics All data are presented as means ± SEM (*n* is indicated in the figures and/or legends). The *t* test was used to define differences between two datasets. To define differences between multiple datasets, two-way ANOVA was used with a Bonferroni multiple comparison post test. The criterion for

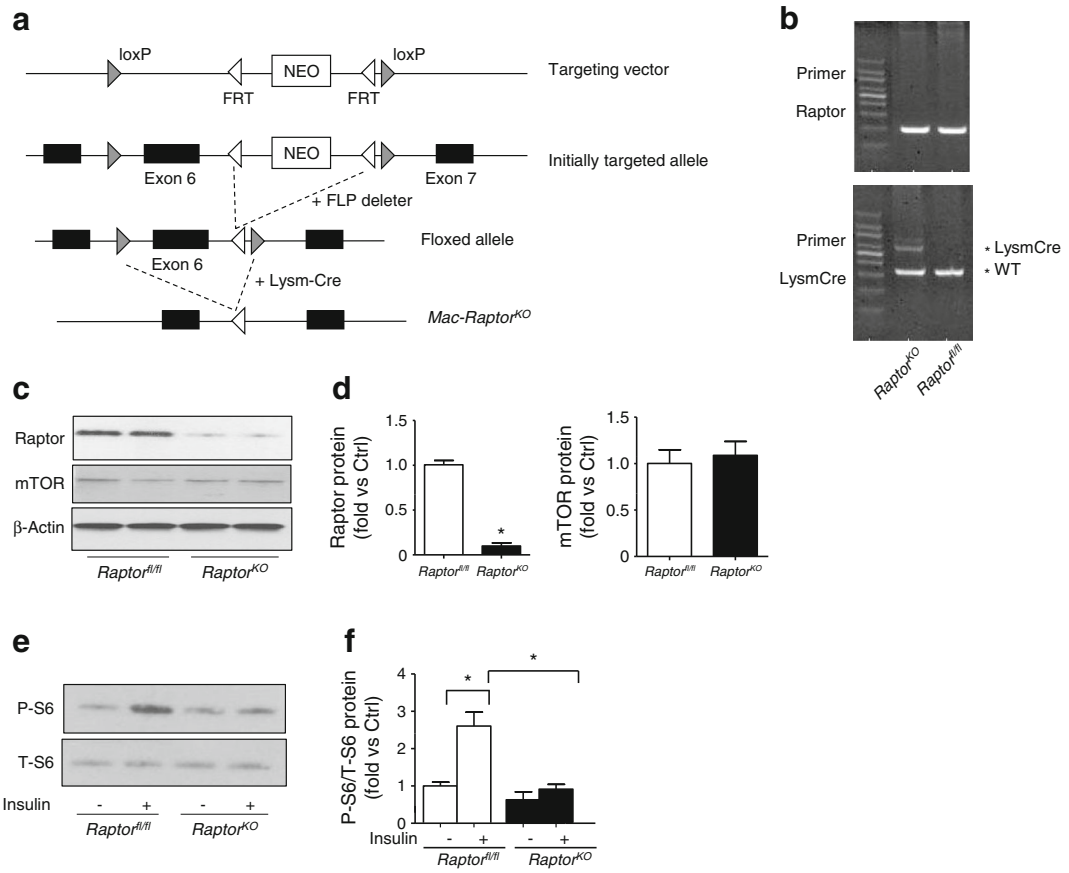

Fig. 1 Generation of *Mac-Raptor*^{KO} mice. (**a**) A targeting vector, containing a NEO selection cassette flanked by flippase-specific FRT sites, and having exon 5 of the *Raptor* gene flanked by loxP site, was used to generate mice with floxed Raptor alleles (*Raptor*$^{flox/flox}$ mice). To generate *Mac-Raptor*^{KO} (*Raptor*^{KO}) mice, *Raptor*$^{flox/flox}$ (*Raptor*$^{fl/fl}$) mice were crossed with Lysm-Cre$^{+/0}$ mice. (**b**) The efficiency of genomic recombination in *Mac-Raptor*^{KO} mice was analysed by PCR. WT, wild type. (**c**) ConA-elicited peritoneal macrophages were isolated from *Raptor*$^{flox/flox}$ and *Mac-Raptor*^{KO} mice. Protein levels of Raptor and total mTOR were measured by western blot. (**d**) Raptor and mTOR were quantified and normalised to *Raptor*$^{flox/flox}$ macrophages. (**e**) BMDMs were isolated from *Raptor*$^{flox/flox}$ and *Mac-Raptor*^{KO} mice. The BMDMs were serum starved for 6 h and treated with serum-free DMEM or with insulin (100 nmol/l) in serum-free DMEM for 30 min. Phospho-S6 ribosomal protein (P-S6) and total S6 (T-S6) were analysed by western blot. (**f**) The ratio of phospho-S6 to total S6 was quantified and normalised to *Raptor*$^{flox/flox}$ macrophages treated with PBS. All data are presented as means ± SEM; n=3–5. *p<0.05, *Raptor*^{KO} vs *Raptor*$^{fl/fl}$ or indicated comparison

significance was set at $p<0.05$. Statistical analyses were performed using GraphPad Prism version 5.01 (GraphPad, San Diego, CA, USA).

Results

Generation of Mac-Raptor^{KO} mice To address the role of macrophage mTORC1 in obesity-related insulin resistance and inflammation in vivo, we generated a mouse model in which the *Raptor* gene was disrupted by homologous recombination in macrophages. Mice with *Raptor* floxed alleles (*Raptor*$^{flox/flox}$ mice) were crossed with transgenic mice expressing Cre recombinase under the control of the Lysm promoter (Fig. 1a), which is highly expressed in macrophages and neutrophils [20]. We employed *Raptor*$^{flox/flox}$*LysmCre*$^{+/0}$ mice as *Mac-Raptor*^{KO} mice and *Raptor*$^{flox/flox}$ as control mice (Fig. 1b). Next, we assessed the efficiency of *Raptor* deletion in *Mac-Raptor*^{KO} macrophages. Raptor protein expression was reduced by >90% in concanavalin A (ConA)-elicited peritoneal macrophages, while the total mTOR level was similar compared with levels in *Raptor*$^{flox/flox}$ controls (Fig. 1c, d). Moreover, macrophage Raptor deficiency abolished the insulin-induced mTORC1 activity in bone marrow-derived macrophages (BMDMs), as shown by decreased S6 phosphorylation (Fig. 1e, f).

Macrophage Raptor deficiency results in improved systemic insulin sensitivity despite similar body mass and adiposity mTORC1 activity is increased in mouse models of obesity and type 2 diabetes, contributing to insulin resistance in a number of cell types [21, 22]. Consistent with previous reports, mTORC1 activity was increased in ConA-elicited peritoneal macrophages of *ob*/*ob* mice and DIO mice (ESM Fig. 1). To assess the role of macrophage mTORC1 in

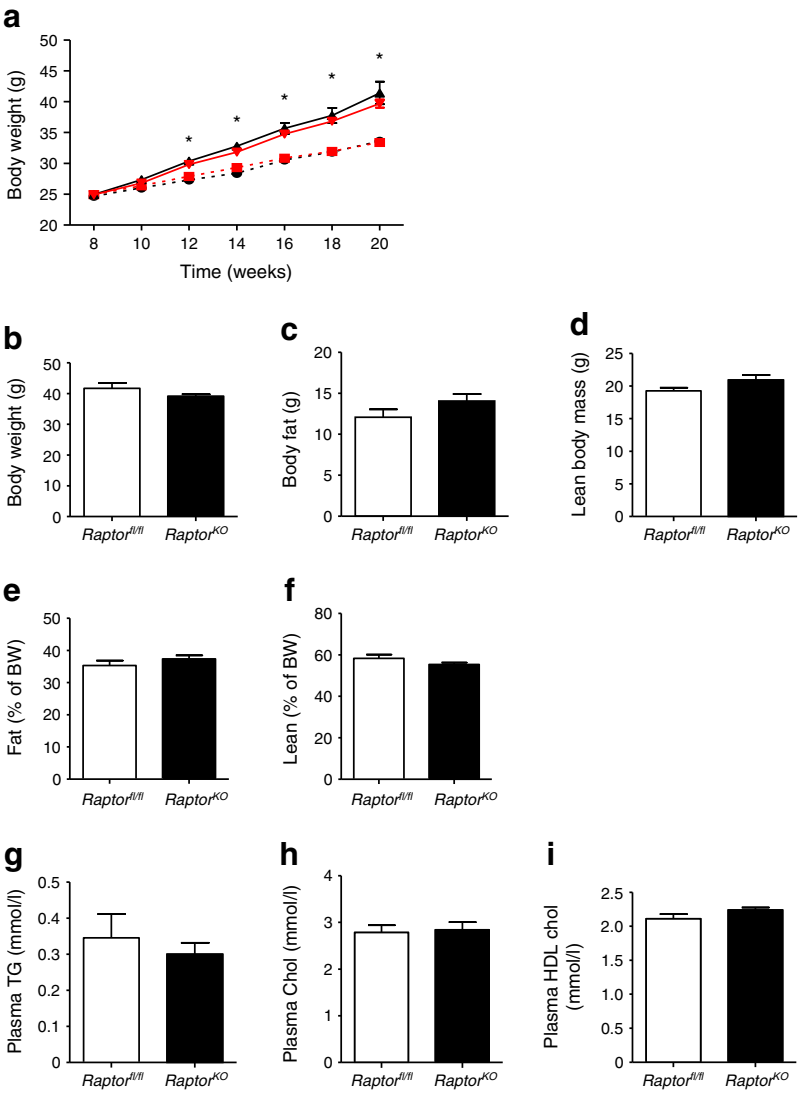

Fig. 2 Macrophage Raptor deficiency did not affect body composition and plasma lipid levels. *Raptor*$^{flox/flox}$ (*Raptor*$^{fl/fl}$) and *Mac-Raptor*^{KO} (*Raptor*^{KO}) mice were fed CD or HFD for 12 weeks. (**a**) Body weight was measured: red dashed line, *Raptor*$^{fl/fl}$ + CD; red unbroken line, *Raptor*$^{fl/fl}$ + HFD; black dashed line, *Raptor*^{KO} + CD; black unbroken line, *Raptor*^{KO} + HFD; *$p<0.05$, CD vs HFD. (**b**–**f**) After 10 weeks of HFD, body weight (**b**), body fat (**c**) and lean body mass (**d**) were measured by NMR and fat (**e**) and lean body mass (**f**) were measured as a percentage of body weight (BW). (**g**–**i**) After 10 weeks of HFD, plasma TG (**g**), cholesterol (Chol) (**h**) and HDL-cholesterol (HDL chol) (**i**) levels were assessed. All data are presented as means ± SEM; $n=5$

regulating systemic insulin sensitivity, we fed *Raptor*$^{flox/flox}$ and *Mac-Raptor*^{KO} mice CD or HFD for 12 weeks. HFD feeding induced body weight gain in mice of both genotypes, without differences between the genotypes (Fig. 2a). Body composition was measured by nuclear magnetic resonance (NMR). Lean weight, body fat and body composition were similar in *Raptor*$^{flox/flox}$ and *Mac-Raptor*^{KO} mice on HFD (Fig. 2b–f). In addition, plasma TG, total cholesterol and HDL-cholesterol levels were similar in the two groups on the HFD (Fig. 2g–i).

Sustained HFD feeding leads to insulin resistance To evaluate the function of macrophage Raptor deficiency in insulin resistance, IPGTTs and ITTs were performed. In the IPGTT plasma glucose and insulin levels were comparable between *Raptor*$^{flox/flox}$ and *Mac-Raptor*^{KO} mice on CD (Fig. 3a–c). After 10 weeks of HFD, *Mac-Raptor*^{KO} mice showed less of an increase in serum glucose at 30 and 60 min after glucose injection compared with their *Raptor*$^{flox/flox}$ controls (Fig. 3a). The AUC for glucose during the IPGTT was reduced by 13%, whereas insulin levels were reduced by 23% at 120 min after glucose injection in HFD-fed *Mac-Raptor*^{KO} compared with *Raptor*$^{flox/flox}$ mice (Fig. 3d, e). Injection of insulin in HFD-fed, but not CD-fed *Mac-Raptor*^{KO} mice, led to an enhanced hypoglycaemic response ($p<0.05$) compared with *Raptor*$^{flox/flox}$ mice, accompanied by a reduction of ~15% in the AUC for glucose (Fig. 3f–h).

We next measured plasma glucose and insulin levels in response to fasting/re-feeding. After 2 h of re-feeding after mice had been fasted overnight, plasma glucose and insulin levels were comparable between *Raptor*$^{flox/flox}$ and *Mac-Raptor*^{KO} mice on the CD (Fig. 4a, b). In contrast, although plasma glucose levels were unchanged in HFD-fed *Mac-Raptor*^{KO} compared with *Raptor*$^{flox/flox}$ mice (Fig. 4c), HFD-fed *Mac-Raptor*^{KO} mice displayed a reduced plasma insulin level after 2 and 4 h of re-feeding (Fig. 4d). These data suggested that a reduction of mTORC1 in macrophages led to improved systemic insulin resistance induced by the HFD.

To understand the mechanisms by which macrophage *Raptor* ablation improved insulin sensitivity, we assessed insulin signalling in the liver, white adipose tissue (WAT) and skeletal muscle. Mice were fed HFD for 12 weeks, and fasted overnight before being administered saline or insulin. We found that the insulin-induced tyrosine phosphorylation of Akt at Ser473 was enhanced in WAT, liver and skeletal muscle of *Raptor*^{KO} mice (Fig. 5a–c), compared with *Raptor*$^{flox/flox}$ mice, consistent with systemically improved insulin sensitivity.

Macrophage Raptor ablation inhibits HFD-induced adipose tissue macrophage accumulation, hepatic steatosis and inflammation The HFD model is known to be associated with hepatic steatosis. Macrophage Raptor deficiency decreased

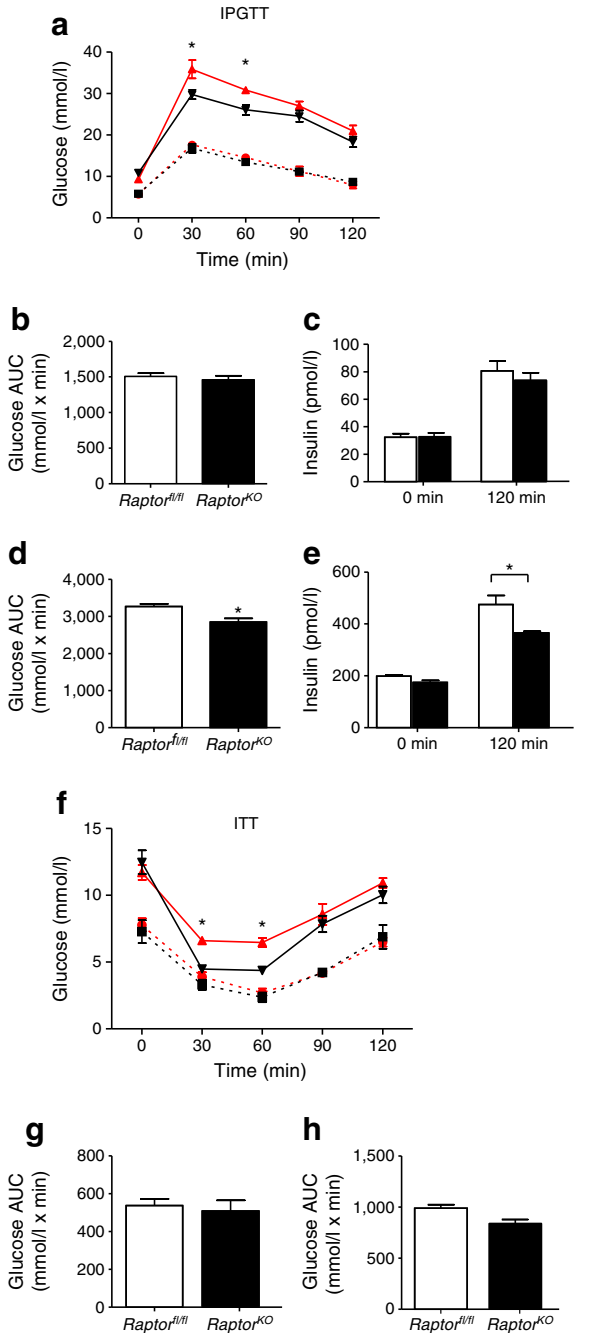

Fig. 3 Insulin resistance was attenuated by macrophage Raptor deficiency. (**a**–**e**) IPGTT was performed after 10 weeks of CD or HFD feeding in *Raptor*$^{flox/flox}$ (*Raptor*$^{fl/fl}$) and *Mac-Raptor*^{KO} (*Raptor*^{KO}) mice. (**a**) Glucose levels were measured: red dashed line, *Raptor*$^{fl/fl}$ + CD; red unbroken line, *Raptor*$^{fl/fl}$ + HFD; black dashed line, *Raptor*^{KO} + CD; black unbroken line, *Raptor*^{KO} + HFD. *$p<0.05$, *Raptor*^{KO} vs *Raptor*$^{fl/fl}$. (**b**) AUC of glucose levels in CD-fed mice. (**c**) Plasma insulin of CD-fed mice was measured at the indicated time points. (**d**) AUC analysis of glucose levels in HFD-fed mice. *$p<0.05$. (**e**) Plasma insulin of HFD-fed mice was measured at the indicated time points. *$p<0.05$ (**f**–**h**) ITT was performed after 10 weeks of CD or HFD feeding in *Raptor*$^{fl/fl}$ and *Mac-Raptor*^{KO} mice. (**f**) Glucose levels were measured: red dashed line, *Raptor*$^{fl/fl}$ + CD; red unbroken line, *Raptor*$^{fl/fl}$ + HFD; black dashed line, *Raptor*^{KO} + CD; black unbroken line, *Raptor*^{KO} + HFD. *$p<0.05$, *Raptor*^{KO} vs *Raptor*$^{fl/fl}$. (**g**, **h**) AUC of glucose levels in CD-fed mice (**g**) or HFD-fed mice (**h**). All data are presented as means ± SEM; $n=5$

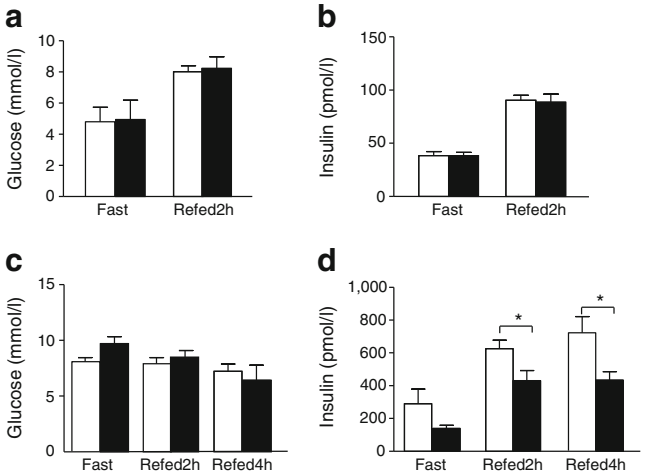

Fig. 4 Plasma insulin level was reduced in *Mac-Raptor*^{KO} mice after re-feeding. Plasma glucose (**a**, **c**) and insulin (**b**, **d**) levels were measured after mice had been fasted overnight (Fast) and after re-feeding for 2 h (Refed2h) or 4 h (Refed4h) in *Raptor*$^{flox/flox}$ (*Raptor*$^{fl/fl}$) and *Mac-Raptor*^{KO} (*Raptor*^{KO}) mice after 11 weeks of CD (**a**, **b**) or HFD (**c**, **d**). All data are presented as means ± SEM; n=5. White bars, *Raptor*$^{fl/fl}$; black bars, *Raptor*^{KO}. *p<0.05, *Raptor*^{KO} vs *Raptor*$^{fl/fl}$

Oil Red O staining in the liver, reflecting decreased lipid accumulation (Fig. 6a), which potentially contributes to the reduced liver to body weight ratio (Fig. 6b). Lipid analysis showed that the hepatic TG levels were significantly decreased in *Mac-Raptor*^{KO} mice (Fig. 6c). The inhibition of hepatic steatosis in *Mac-Raptor*^{KO} mice was associated with reduced mRNA expression of the macrophage marker *Cd68* and the inflammatory cytokines *Tnf* and *Ccl2* (but not *Il10*), in the liver (Fig. 6d–g). When WAT was examined, we found that macrophage Raptor deficiency decreased the F4/80-positive staining (Fig. 6h), reflecting the content of adipose tissue macrophages (ATMs) and the mRNA expression of macrophage marker *Cd68* (50% and 52% reduction, respectively) (Fig. 6i, j), suggesting decreased ATM accumulation. ATMs are reported to consist of at least two types, referred to as classically activated M1 and alternatively activated M2 macrophages [23]. The expressions of all M1 markers measured were downregulated by macrophage Raptor deficiency. For example, the mRNA level of inflammatory cytokines *Tnf*, *Ccl2* and *iNOS* (also known as *Nos2*) was reduced by 63%, 47% and 75%, respectively (Fig. 6k, l, o). On the other hand, the M2 marker *Arg1* was increased by macrophage Raptor deficiency (Fig. 6n) and *Il10* was unchanged (Fig. 6m). The ratio of *iNOS/Arg1* was reduced by 84% (Fig. 6p), suggesting M2 polarisation, as described previously [24].

Raptor deletion in macrophages inhibits inflammatory gene expression via the IRE1α/JNK/NFκB pathway in the HFD model Our finding that macrophage Raptor deficiency resulted in decreased inflammation in the liver and adipose tissue led us to hypothesise that mTORC1 may play a role in controlling macrophage inflammation in response to HFD challenge. To investigate the role of mTORC1 in macrophage

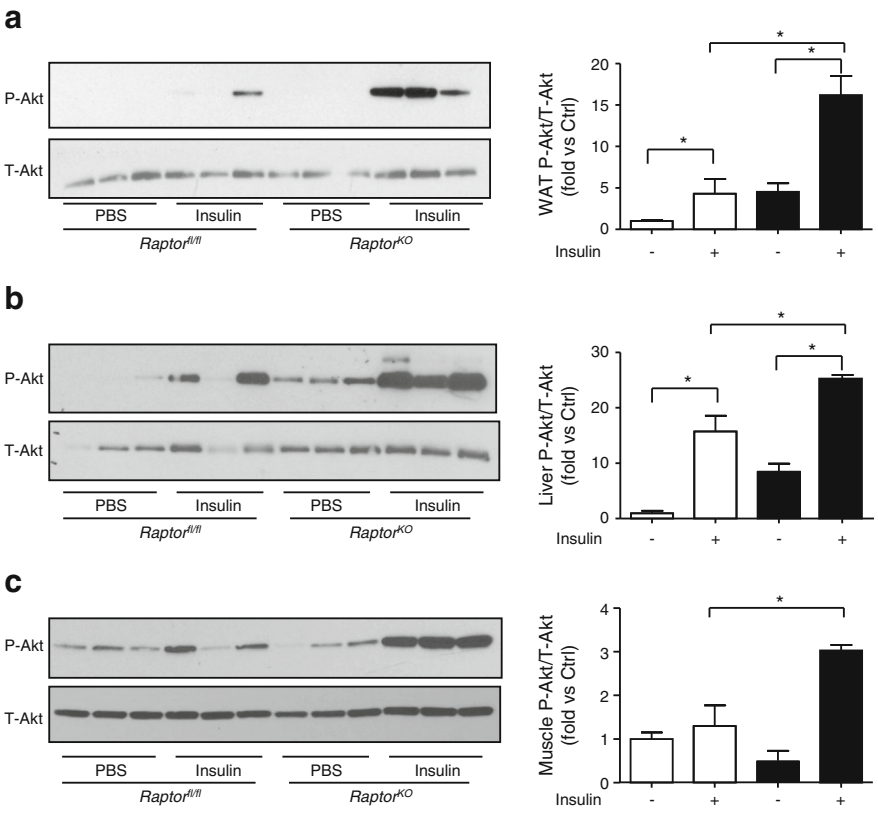

Fig. 5 Insulin sensitivity was improved by macrophage Raptor deficiency. *Raptor*$^{flox/flox}$ (*Raptor*$^{fl/fl}$) and *Mac-Raptor*^{KO} (*Raptor*^{KO}) mice fed HFD for 12 weeks were injected with PBS or insulin (0.75 U/kg body weight). At 10 min after injection, the levels of phospho-AktSer473 (P-Akt) and total-Akt (T-Akt) in WAT (**a**), liver (**b**) and muscle (**c**) were measured by western blot and the ratio of P-Akt to T-Akt was quantified. All data are presented as means ± SEM; n=5. White bars, *Raptor*$^{fl/fl}$; black bars, *Raptor*^{KO}. *p<0.05 for indicated comparisons

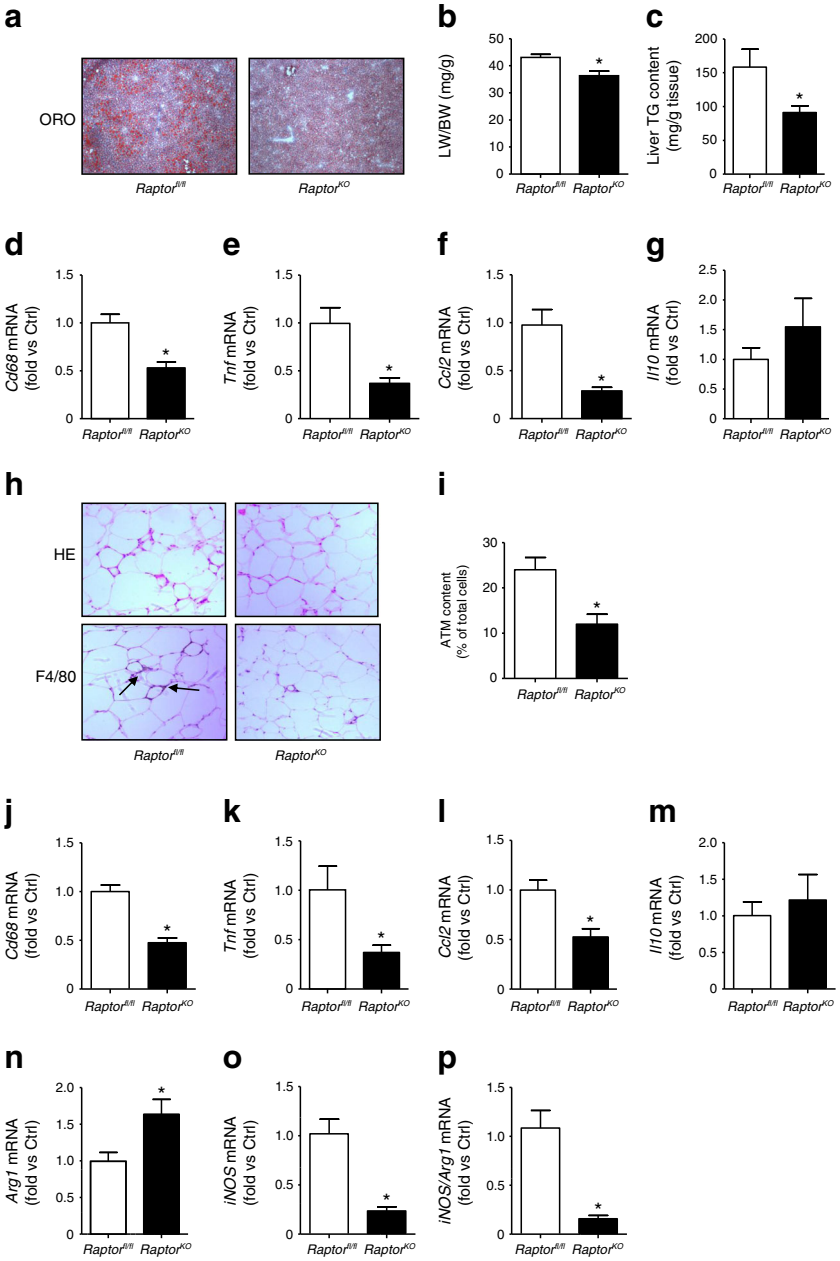

Fig. 6 Macrophage Raptor deficiency results in reduced macrophage inflammatory activation in adipose tissue and liver. (**a**) Oil red O (ORO) staining was performed in liver (magnification ×40). (**b**) The ratio of liver weight and body weight (LW/BW). (**c**) Liver TG content was measured and normalised to liver weight. (**d**–**g**) mRNA expression of macrophage markers *Cd68* and inflammatory factors *Tnf*, *Ccl2* and *Il10* in liver of HFD-fed *Raptor*$^{\text{flox/flox}}$ (*Raptor*$^{\text{fl/fl}}$) and *Mac-Raptor*$^{\text{KO}}$ (*Raptor*$^{\text{KO}}$) mice. (**h**) Haematoxylin and eosin (HE) and F4/80 staining of adipose tissue (magnification ×100). (**i**) ATMs as percentage of total cells depicted in (**h**). (**j**–**p**) mRNA levels of macrophage markers *Cd68*, and M1 and M2 markers in adipose tissue of HFD-fed *Raptor*$^{\text{fl/fl}}$ and *Mac-Raptor*$^{\text{KO}}$ mice were measured by quantitative PCR. Data are presented as means ± SEM; $n=5$. *$p<0.05$, *Raptor*$^{\text{KO}}$ vs *Raptor*$^{\text{fl/fl}}$

inflammation in HFD-fed mice, we isolated ConA-elicited peritoneal macrophages from *Raptor*$^{\text{flox/flox}}$ and *Mac-Raptor*$^{\text{KO}}$ mice fed CD or HFD for 12 weeks, and analysed signalling pathways downstream of mTORC1 immediately after macrophage isolation.

HFD increased mTORC1 activity, assessed by phosphorylation of S6, in *Raptor*$^{\text{flox/flox}}$, but not in *Mac-Raptor*$^{\text{KO}}$ macrophages (Fig. 7a). Our previous study showed that ER stress was activated by long-term mTORC1 activation in liver [18]. We thus investigated the role of macrophage *Raptor* in ER stress. HFD activated the ER stress branches PERK and ATF6 in both *Raptor*$^{\text{flox/flox}}$ and *Mac-Raptor*$^{\text{flox/flox}}$ macrophages, reflected by increased phosphorylation of eukaryotic translation initiation factor 2α (eIF2α) and nuclear ATF6, respectively (Fig. 7a–c). Interestingly, the HFD-induced activation of IRE1α branch, reflected by XBP1 splicing, was much more dramatic in *Raptor*$^{\text{flox/flox}}$ than in *Mac-Raptor*$^{\text{KO}}$ macrophages (Fig. 7d), suggesting that this ER stress branch may be modulated by mTORC1 activity.

mTORC1 exerts negative feedback regulation on Akt activation [21, 25]. To test whether Akt was involved in mTORC1-triggered IRE1α activation, we measured Akt activity. Phospho-Akt levels were decreased in macrophages from *Raptor*$^{\text{flox/flox}}$ mice on HFD compared with those on CD, while this suppression of Akt was rescued by macrophage Raptor deficiency (Fig. 7e, f). In *Raptor*$^{\text{flox/flox}}$

macrophages, the suppression of Akt was inversely correlated with phosphorylation of JNK and NF-κB (P65), and recovery of Akt phosphorylation by Raptor deficiency was associated with blunted JNK and P65 activation (Fig. 7g, h). Paralleling the decreased level of phospho-JNK and phospho-P65, the mRNA levels of inflammatory genes in HFD-fed mice were reduced by macrophage Raptor deficiency (Fig. 7i, j).

Raptor ablation or mTORC1 inhibition by rapamycin decreases the inflammatory response to palmitic acid via the IRE1α/JNK-NFκB pathway Recent evidence points to the importance of SFAs, such as palmitic acid, which are systemically elevated in DIO and induce insulin resistance by activation of intracellular inflammatory signalling pathways [26, 27]. We thus investigated whether Raptor deficiency affected the inflammatory response to palmitic acid in macrophages. Since rapamycin also inhibits mTORC1, we investigated the effects of rapamycin on inflammatory gene expression in macrophages concomitantly. BMDMs were isolated from *Mac-Raptor*^{KO} and *Raptor*$^{flox/flox}$ mice and challenged with palmitic acid. Concomitantly, BMDMs from *Raptor*$^{flox/flox}$ mice were pre-treated with rapamycin followed by a palmitic acid challenge. Palmitic acid induced mTORC1 activity, assessed by phosphorylation of S6 in *Raptor*$^{flox/flox}$ macrophages, and this response was blunted by rapamycin (Fig. 8a, b) and by macrophage Raptor deficiency

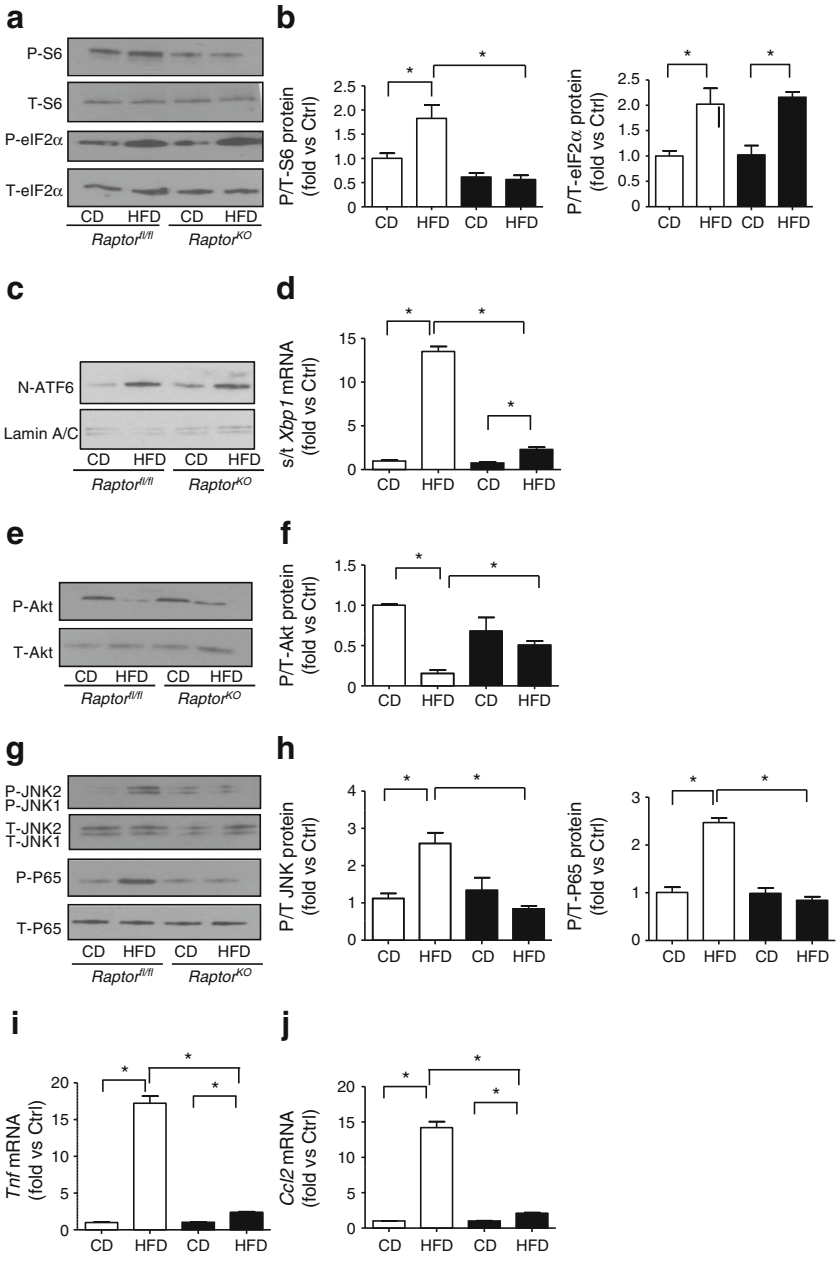

Fig. 7 Macrophage Raptor deficiency suppressed the HFD-induced IRE1α/JNK/NF-κB pathway by increasing Akt phosphorylation. ConA-elicited macrophages were isolated from *Raptor*$^{flox/flox}$ (*Raptor*$^{fl/fl}$) and *Mac-Raptor*^{KO} (*Raptor*^{KO}) mice fed CD or HFD for 12 weeks. (**a**) Western blot of phosphorylated (P-) and total (T-) S6 and eIF2α. (**b**) Ratio of indicated phosphorylated to total protein (P/T) in (**a**), normalised to *Raptor*$^{fl/fl}$ mice on CD. (**c**) Western blot of nuclear (N-) ATF6 and lamin A/C. (**d**) mRNA expression of spliced and total *Xbp1* was measured by quantitative PCR. The ratio of spliced (s) and total (t) *Xbp1* mRNA was calculated. (**e**–**h**) Western blot was performed to measure P- and T- Akt (**e**), JNK and P65 (**g**). The ratio of phosphorylated to total protein (P/T) for (**e**) and (**g**) was normalised to *Raptor*$^{fl/fl}$ on CD (**f** and **h**). (**i**, **j**) mRNA expression of *Tnf* and *Ccl2* was measured by quantitative PCR. Data are presented as means ± SEM; $n=5$. White bars, *Raptor*$^{fl/fl}$; black bars, *Raptor*^{KO}. *$p<0.05$ for indicated comparisons

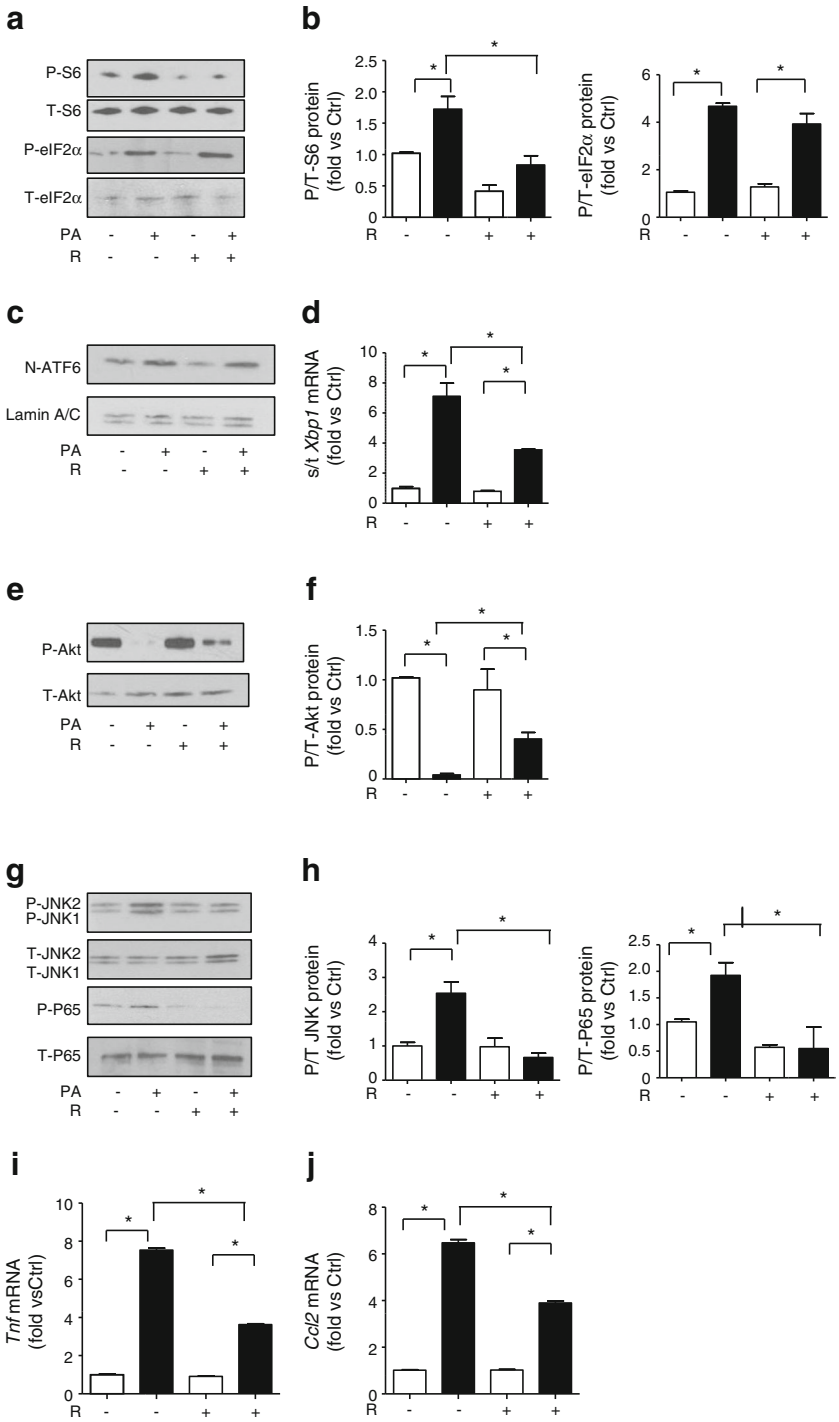

Fig. 8 Rapamycin suppressed the palmitic acid-induced IRE1α/JNK/NF-κB pathway by increasing Akt phosphorylation. BMDMs were isolated from *Raptor*$^{flox/flox}$ (*Raptor*$^{fl/fl}$) mice, pre-incubated with or without rapamycin (R, 100 nmol/l) for 30 min and treated with BSA or BSA-conjugated palmitic acid (PA, 0.5 mmol/l) for 4 h. (**a**) Western blot of phosphorylated (P-) and total (T-) S6 and eIF2α. (**b**) Ratio of indicated phosphorylated and total protein (P/T) in (**a**), and normalised to *Raptor*$^{fl/fl}$ BMDMs treated with BSA. (**c**) Western blot of nuclear (N-) ATF6 and lamin A/C. (**d**) mRNA expression of spliced (s) and total (t) *Xbp1*. The ratio of spliced and total *Xbp1* was calculated. (**e**–**h**) Western blot of P- and total T- Akt (**e**), JNK and P65 (**g**). The ratio of indicated phosphorylated and total protein (P/T) in (**e**) and (**g**) was normalised to *Raptor*$^{fl/fl}$ treated with BSA (**f**, **h**). (**i**, **j**) mRNA expression of *Tnf* and *Ccl2*. Data are presented as means ± SEM; $n=3$. White bars, BSA; black bars, palmitic acid. *$p<0.05$ for the indicated comparisons

(ESM Fig. 2a, b). Palmitic acid induced the activation of all three ER stress pathways, including PERK, ATF6 and IRE1α in *Raptor*$^{flox/flox}$ macrophages, reflected by increased phospho-eIF2α, nuclear ATF6 and XBP-1 splicing, respectively (Fig. 8a–d and ESM Fig. 2a–d). Consistent with the in vivo results, only the activation of the IRE1α pathway was decreased by the mTORC1 inhibitor rapamycin (Fig. 8c, d) and by Raptor deficiency (ESM Fig. 2c, d). Moreover, the repression of phospho-Akt by palmitic acid was attenuated by rapamycin (Fig. 8e, f) and by Raptor deficiency (ESM Fig. 2e, f), inversely correlated with the changes in levels of phospho-JNK, phospho-P65, *Tnf* mRNA and *Ccl2* mRNA (Fig. 8g–j and ESM Fig. 2g–l). These observations thus confirmed our in vivo findings, indicating that Akt-mediated IRE1α activation plays a crucial role in mTORC1-triggered inflammation.

Discussion

In recent decades, local inflammation was found to be important in the suppression of insulin signalling pathways and insulin resistance [28]. The mTORC1 pathway, activated in obesity, is responsive to type 2 diabetes and insulin resistance partly via ER stress pathways [18, 29]. It has been shown that inhibition of mTOR by rapamycin promotes production of proinflammatory cytokines and blocks the release of IL-10 in human monocytes and mouse macrophages in response to endotoxin, suggesting that mTOR is anti-inflammatory [30–33]. However, it is unclear whether macrophage mTORC1 is involved in the development of insulin resistance. Surprisingly, in the present report, we found that macrophage mTORC1 has a proinflammatory role in diet-induced insulin resistance. Our studies produced two main findings: (1) macrophage Raptor deficiency improved systemic insulin sensitivity, although body composition was unchanged; (2) macrophage Raptor deficiency suppressed the activation of JNK and NF-κB pathways by rescuing Akt and selectively repressing IRE1α in response to HFD and palmitic acid (schematically shown in Fig. 9).

A novel finding of this study is that macrophage Raptor deficiency decreased insulin resistance by markedly suppressing the local inflammatory response to HFD. We showed that the HFD-impaired insulin sensitivity was improved by macrophage Raptor deficiency. In addition, macrophage Raptor deficiency dramatically blocked the HFD-induced activation of mTORC1 activity. Moreover, this protection also included significant reduction in hepatic steatosis and adipose tissue macrophage accumulation. Since the polarisation of macrophages in adipose tissue is important for obesity and insulin resistance [23], we studied M1/M2 markers. Consistent with findings from studies by Byles et al [24], macrophage Raptor deficiency decreased the mRNA levels of several M1 inflammatory genes, such as *Tnf* and *Ccl2*, in WAT, and increased the M2 polarisation marker *Arg1*. Although the precise role of macrophage polarisation in mediating insulin resistance remains incompletely defined, ATMs were found to be responsible for almost all adipose tissue TNF-α expression, and neutralisation of TNF-α in obese rats caused improved peripheral uptake of glucose [1, 8]. Our study suggested that macrophage Raptor deficiency decreased insulin resistance by attenuating macrophage inflammation. Our results seem to be in conflict with those from Weichart et al, who reported that mTORC1 inhibition by rapamycin increased the production of proinflammatory cytokines in monocytes and macrophages [30]. However, in contrast to Raptor deficiency, long-term rapamycin treatment also inhibits mTORC2 assembly and Akt signalling, as has been shown in several cell lines [34], which may explain the discrepancy between our study and that of Weichart et al.

In addition, our study indicated the existence of an mTORC1–Akt feedback loop. Macrophage Raptor deficiency reversed the loss of Akt-mediated IRE1α inhibition and, consequently, JNK and NF-κB activation. The possible mechanism of the selective inhibition of IRE1α by Akt might be through TRAF2 and Bcl-2 family members. As Hu et al and Kato et al have shown, activation of Akt downregulates expression of TRAF2, which is an adaptor protein that couples IRE1α to JNK and NF-κB activation [35], whereas inhibition of Akt increased TRAF2 [36]. In addition to TRAF2, Bcl-2 family members, such as Bax and Bcl-2 homology domain 3 (BH3)-only proteins, which were inhibited by Akt, directly modified IRE1α activity [37, 38]. Moreover, the decreased expression of a downstream target of IRE1α, spliced *Xbp1,* may also contribute to the anti-inflammatory effect of macrophage Raptor deficiency, as it has been shown to be required for the TLR signalling-related production of proinflammatory cytokines such as TNF-α and chemokine (C-C motif) ligand 2 [39, 40].

In summary, our results demonstrate that macrophage mTORC1 is important in regulating HFD-induced insulin resistance by modulation of the inflammatory response. Treatment with the immunosuppressive drug rapamycin effectively attenuated inflammation [41]. However, long-term administration of rapamycin induced insulin resistance, which was mediated by mTORC2 loss [42] and hyperlipidaemia [43]. Different from long-term rapamycin treatment, our study showed that genetic disruption of mTORC1 in macrophages attenuated the inflammatory response and further improved insulin sensitivity, which could potentially have a beneficial effect in insulin resistance.

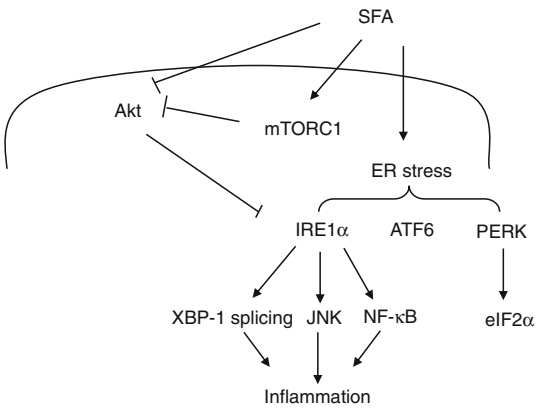

Fig. 9 The proinflammatory role of mTORC1 in SFA-induced inflammation. mTORC1 is activated by palmitic acid, leading to suppression of Akt phosphorylation. As Akt suppresses activation of IRE1α, mTORC1-mediated inhibition of Akt causes selective activation of the IRE1α/JNK/NF-κB pathway and induces inflammation

Acknowledgements The authors would like to thank A. Tall, Columbia University, New York, NY, USA, for his advice and help on experimental design and manuscript writing.

Funding DA is supported by the National Natural Science Foundation of China (Nos 81322006 and 81370396). YZ is supported by the Major National Basic Research Grant of China (No. 2010CB912504). MW is supported by The Netherlands Organization of Scientific Research (NWO VENI – grant 916.11.072).

Duality of interest The authors declare that there is no duality of interest associated with this manuscript.

Contribution statement HJ contributed to the concept and design, data acquisition, analysis and interpretation and drafting of the article. MW contributed to the concept and design, data acquisition and revision of the article. CW and YZ contributed to the data acquisition and analysis and revision of the article. DA contributed to the concept and design, data acquisition, analysis and interpretation of data and revision of the article. DA is the guarantor of the work. All authors approved the final version.

References

1. Hotamisligil GS, Shargill NS, Spiegelman BM (1993) Adipose expression of tumor necrosis factor-alpha: direct role in obesity-linked insulin resistance. Science 259:87–91
2. Flegal KM, Graubard BI, Williamson DF, Gail MH (2007) Cause-specific excess deaths associated with underweight, overweight, and obesity. JAMA 298:2028–2037
3. Ozcan U, Cao Q, Yilmaz E et al (2004) Endoplasmic reticulum stress links obesity, insulin action, and type 2 diabetes. Science 306:457–461
4. Park SW, Zhou Y, Lee J et al (2010) The regulatory subunits of PI3K, p85alpha and p85beta, interact with XBP-1 and increase its nuclear translocation. Nat Med 16:429–437
5. Ozcan L, Ergin AS, Lu A et al (2009) Endoplasmic reticulum stress plays a central role in development of leptin resistance. Cell Metab 9: 35–51
6. Obstfeld AE, Sugaru E, Thearle M et al (2010) C-C chemokine receptor 2 (CCR2) regulates the hepatic recruitment of myeloid cells that promote obesity-induced hepatic steatosis. Diabetes 59:916–925
7. Qatanani M, Lazar MA (2007) Mechanisms of obesity-associated insulin resistance: many choices on the menu. Genes Dev 21:1443–1455
8. Weisberg SP, McCann D, Desai M, Rosenbaum M, Leibel RL, Ferrante AW Jr (2003) Obesity is associated with macrophage accumulation in adipose tissue. J Clin Invest 112:1796–1808
9. Han MS, Jung DY, Morel C et al (2013) JNK expression by macrophages promotes obesity-induced insulin resistance and inflammation. Science 339:218–222
10. Solinas G, Vilcu C, Neels JG et al (2007) JNK1 in hematopoietically derived cells contributes to diet-induced inflammation and insulin resistance without affecting obesity. Cell Metab 6:386–397
11. Boden G (2002) Interaction between free fatty acids and glucose metabolism. Curr Opin Clin Nutr Metab Care 5:545–549
12. Nguyen MT, Favelyukis S, Nguyen AK et al (2007) A subpopulation of macrophages infiltrates hypertrophic adipose tissue and is activated by free fatty acids via Toll-like receptors 2 and 4 and JNK-dependent pathways. J Biol Chem 282:35279–35292
13. Seimon TA, Nadolski MJ, Liao X et al (2010) Atherogenic lipids and lipoproteins trigger CD36-TLR2-dependent apoptosis in macrophages undergoing endoplasmic reticulum stress. Cell Metab 12: 467–482
14. Erbay E, Babaev VR, Mayers JR et al (2009) Reducing endoplasmic reticulum stress through a macrophage lipid chaperone alleviates atherosclerosis. Nat Med 15:1383–1391
15. Kapahi P, Chen D, Rogers AN et al (2010) With TOR, less is more: a key role for the conserved nutrient-sensing TOR pathway in aging. Cell Metab 11:453–465
16. Wullschleger S, Loewith R, Hall MN (2006) TOR signaling in growth and metabolism. Cell 124:471–484
17. Ozcan U, Ozcan L, Yilmaz E et al (2008) Loss of the tuberous sclerosis complex tumor suppressors triggers the unfolded protein response to regulate insulin signaling and apoptosis. Mol Cell 29: 541–551
18. Ai D, Baez JM, Jiang H et al (2012) Activation of ER stress and mTORC1 suppresses hepatic sortilin-1 levels in obese mice. J Clin Invest 122:1677–1687
19. Hotamisligil GS (2010) Endoplasmic reticulum stress and the inflammatory basis of metabolic disease. Cell 140:900–917
20. Jakubzick C, Bogunovic M, Bonito AJ, Kuan EL, Merad M, Randolph GJ (2008) Lymph-migrating, tissue-derived dendritic cells are minor constituents within steady-state lymph nodes. J Exp Med 205:2839–2850
21. Manning BD (2004) Balancing Akt with S6K: implications for both metabolic diseases and tumorigenesis. J Cell Biol 167:399–403
22. Tremblay F, Brule S, Hee Um S et al (2007) Identification of IRS-1 Ser-1101 as a target of S6K1 in nutrient- and obesity-induced insulin resistance. Proc Natl Acad Sci U S A 104:14056–14061
23. Lumeng CN, Bodzin JL, Saltiel AR (2007) Obesity induces a phenotypic switch in adipose tissue macrophage polarization. J Clin Invest 117:175–184
24. Byles V, Covarrubias AJ, Ben-Sahra I et al (2013) The TSC-mTOR pathway regulates macrophage polarization. Nat Commun 4:2834
25. Zhang HH, Lipovsky AI, Dibble CC, Sahin M, Manning BD (2006) S6K1 regulates GSK3 under conditions of mTOR-dependent feedback inhibition of Akt. Mol Cell 24:185–197
26. Kim JK (2006) Fat uses a TOLL-road to connect inflammation and diabetes. Cell Metab 4:417–419
27. Shi H, Kokoeva MV, Inouye K, Tzameli I, Yin H, Flier JS (2006) TLR4 links innate immunity and fatty acid-induced insulin resistance. J Clin Invest 116:3015–3025
28. Sabio G, Davis RJ (2010) cJun NH2-terminal kinase 1 (JNK1): roles in metabolic regulation of insulin resistance. Trends Biochem Sci 35: 490–496
29. Laplante M, Sabatini DM (2009) mTOR signaling at a glance. J Cell Sci 122:3589–3594
30. Weichhart T, Costantino G, Poglitsch M et al (2008) The TSC-mTOR signaling pathway regulates the innate inflammatory response. Immunity 29:565–577
31. Weichhart T, Haidinger M, Katholnig K et al (2011) Inhibition of mTOR blocks the anti-inflammatory effects of glucocorticoids in myeloid immune cells. Blood 117:4273–4283
32. Katholnig K, Kaltenecker CC, Hayakawa H et al (2013) p38alpha senses environmental stress to control innate immune responses via mechanistic target of rapamycin. J Immunol 190:1519–1527
33. Weichhart T, Saemann MD (2009) The multiple facets of mTOR in immunity. Trends Immunol 30:218–226
34. Sarbassov DD, Ali SM, Sengupta S et al (2006) Prolonged rapamycin treatment inhibits mTORC2 assembly and Akt/PKB. Mol Cell 22: 159–168
35. Hu P, Han Z, Couvillon AD, Kaufman RJ, Exton JH (2006) Autocrine tumor necrosis factor alpha links endoplasmic reticulum stress to the membrane death receptor pathway through IRE1alpha-mediated NF-kappaB activation and down-regulation of TRAF2 expression. Mol Cell Biol 26:3071–3084
36. Kato H, Nakajima S, Saito Y, Takahashi S, Katoh R, Kitamura M (2012) mTORC1 serves ER stress-triggered apoptosis via selective activation of the IRE1-JNK pathway. Cell Death Differ 19:310–320
37. Hetz C, Bernasconi P, Fisher J et al (2006) Proapoptotic BAX and BAK modulate the unfolded protein response by a direct interaction with IRE1alpha. Science 312:572–576

38. Gardai SJ, Hildeman DA, Frankel SK et al (2004) Phosphorylation of Bax Ser184 by Akt regulates its activity and apoptosis in neutrophils. J Biol Chem 279:21085–21095
39. Zeng L, Liu YP, Sha H, Chen H, Qi L, Smith JA (2010) XBP-1 couples endoplasmic reticulum stress to augmented IFN-beta induction via a cis-acting enhancer in macrophages. J Immunol 185:2324–2330
40. Martinon F, Chen X, Lee AH, Glimcher LH (2010) TLR activation of the transcription factor XBP1 regulates innate immune responses in macrophages. Nat Immunol 11:411–418
41. Chen WQ, Zhong L, Zhang L et al (2009) Oral rapamycin attenuates inflammation and enhances stability of atherosclerotic plaques in rabbits independent of serum lipid levels. Br J Pharmacol 156:941–951
42. Lamming DW, Ye L, Katajisto P et al (2012) Rapamycin-induced insulin resistance is mediated by mTORC2 loss and uncoupled from longevity. Science 335:1638–1643
43. Ai D, Chen C, Han S et al (2012) Regulation of hepatic LDL receptors by mTORC1 and PCSK9 in mice. J Clin Invest 122:1262–1270